

Calculation of the Tooth Root Load Carrying Capacity of Beveloid Gears

C. Brecher, M. Brumm and J. Henser

In this paper, two developed methods of tooth root load carrying capacity calculations for beveloid gears with parallel axes are presented, in part utilizing WZL software *GearGenerator* and *ZaKo3D*. One method calculates the tooth root load-carrying capacity in an FE-based approach. For the other, analytic formulas are employed to calculate the tooth root load-carrying capacity of beveloid gears. To conclude, both methods are applied to a test gear. The methods are compared both to each other and to other tests on beveloid gears with parallel axes in test bench trials.

Introduction and Challenge

A particular gear type which becomes more and more important is the beveloid gear, also known as conical involute gear. This is mainly due to their ability to realize small crossing angles between shafts and they can be produced economically on conventional gear grinding machines (Refs. 1–2). Beveloid gears have been used in marine applications, for example, for many years (Refs. 3–5). In recent years the use of beveloid gears in the automotive sector has increased (Refs. 6–7). Here the beveloid gear is used, for example in four wheel drives to transmit torque and rotation from the output of the gearbox to a front axle that may not be parallel.

Geometrical characteristics of beveloid gears. Beveloid gears are used to transmit torque and rotation between elements of crossing, skew or parallel axes (Ref. 6). The geometry of beveloid gears is derived from cylindrical spur or helical gears. The base circle and the pitch circle of beveloids are cylindrical, as presented in the middle section of Figure 1. The pitch and the module are constant along the tooth width. The difference between beveloid gears and cylindrical gears is the varying profile shift along the tooth width to realize crossed or skew axes. For realizing the varying profile shift, the root cone angle θ_f is defined which is generated during gear cutting and gear grinding by a change of the feed during the process. The form of the tip of a beveloid gear is usually conical. The tip cone angle θ_a is determined by the geometry of the workpiece.

A special use of beveloid gears is the arrangement with parallel axes. This is real-

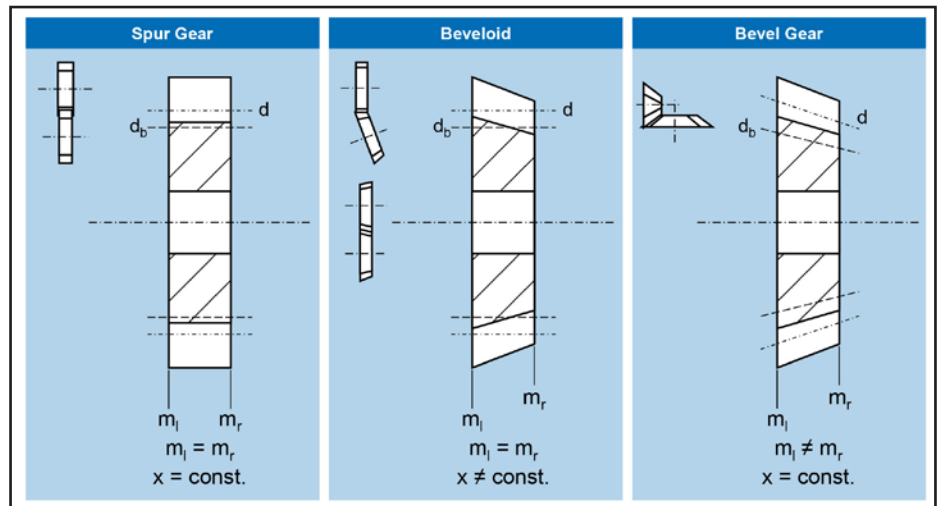


Figure 1 Geometrical characteristics of beveloid gears (Ref. 2).

ized by two meshing beveloids that have a cone angle θ of the same absolute value but with opposite orientation (Ref. 2).

Another gear type which is used for realizing crossing or skew axes is the bevel gear. Bevel gears have a conical pitch and base envelope. This results in a varying module m along the tooth width (Ref. 2). Beveloids are usually preferred to bevel gears when small crossing angles must be realized due to manufacturing limits of bevel gears. This is related to the long cone distances of gears with small cone angles which require substantial dimensions of the bevel gear cutting machine (Ref. 8).

Contact behavior of beveloid gears. Beveloid gears can be mounted with parallel, crossed or skew axes. The axis orientation has substantial influence on the gear mesh (Fig. 2). In Figure 2 (left) a typical contact pattern of beveloid with parallel axes is presented. The contact

pattern is spread over the whole flank. On the right side of Figure 2 a typical contact pattern of beveloid gears with crossed axes is illustrated. Two involute beveloid gears with crossed axes have point contact. The resulting contact pattern is narrower than the contact pattern of beveloid gears with parallel axes. To achieve a full contact pattern of beveloid gears with crossed or skew axes at least one gear has to be designed with non-involute flanks. In this case, the manufacturing with standard methods like generating grinding is no longer possible. For some applications beveloid gears with conjugated flanks are manufactured by topological grinding to achieve nearly full contact (Ref. 6) but for most applications this manufacturing method is avoided for economic reasons.

Challenge. To achieve a high power/weight ratio, a precise calculation of the gear load and load carrying capac-

ity is necessary to design gears in an economical way. At the state of the art, no approved method for the tooth root load carrying capacity calculation for beveloid gears exists. Therefore the beveloid gear is approximated by a substitute spur gear with the gear data of the middle transverse section of the beveloid gear. The imprecision of this method is shown in Figure 3.

In the diagrams the tooth root stresses of a beveloid gear and a substitute spur gear are compared. The beveloid gear has an axis angle of 7.2° . The substitute spur gear is derived from the gear data of the middle transverse section of the beveloid gear. It can be seen that the stresses of the beveloid are significant higher. Reasons for this are the different root fillet geometry and the different contact behavior. Thus the calculation of the tooth root load carrying capacity of beveloid gears with a substitute spur gear according to existing standards for cylindrical gears is not possible without further ado.

A more precise calculation method can lead to a better design of beveloid gears with a higher power/weight ratio. Furthermore no simulation method for the running behavior of beveloid gears with and without load exists. Such a method could determine the tooth root load carrying capacity for a large number of variants in a short time. Therefore the project "Development and Verification of a Method to Calculate the Tooth Root Load-Carrying Capacity of Beveloid Gears," which is sponsored by the German research funding organization Deutsche Forschungsgemeinschaft (DFG), has been initialized.

Objective and Approach

In this paper the development of two calculation methods for the tooth root load carrying capacity of beveloid gears with parallel axes is described. In Error! Reference source not found, the approach for the development of these methods is illustrated. The initial point is the determination of the tooth root fatigue strength of beveloid gears on a test rig. The results are used to validate a local based calculation method to calculate the tooth root load carrying capacity of beveloid gears.

The initial step of the local based calculation method is the manufacturing simulation with the WZL software

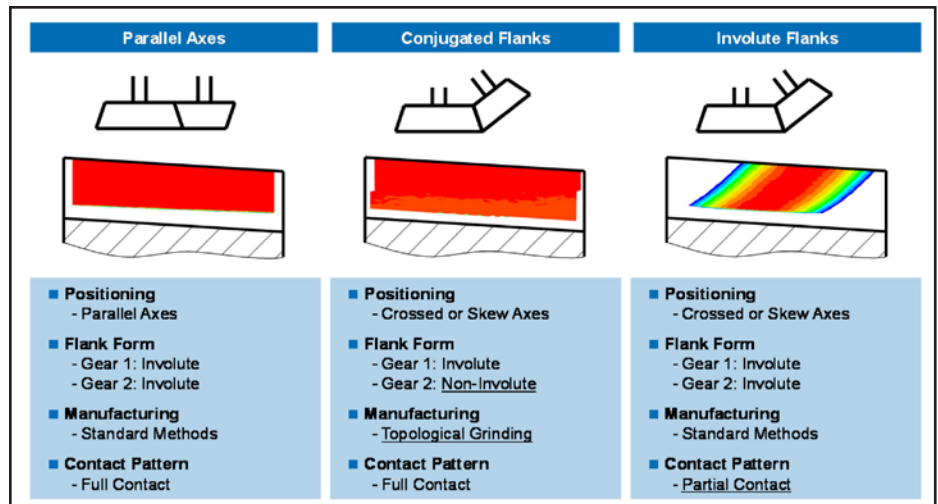


Figure 2 Contact characteristics of beveloid gears.

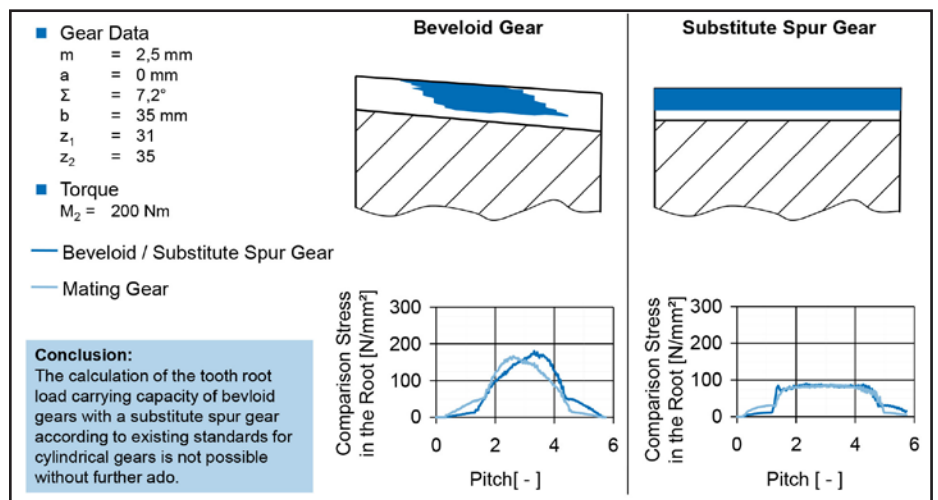


Figure 3 Comparison of the tooth root stresses of a beveloid gear and its substitute cylindrical gear.

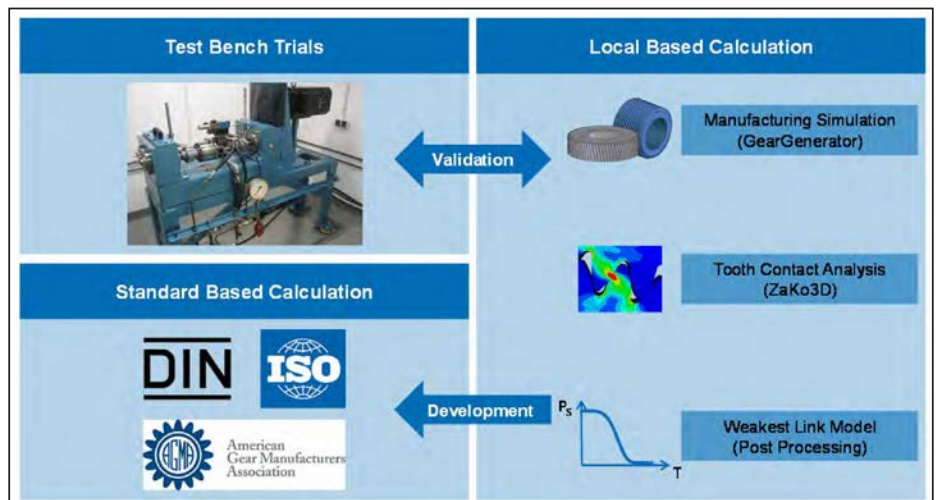


Figure 4 Approach for developing calculation methods for tooth root load carrying capacity of beveloid gears.

GearGenerator. In the manufacturing simulation, a 3D geometry of the beveloid gear is created by simulating the generating grinding process (Refs. 1, 9). The resulting beveloid geometries are used in an FE-based tooth contact analysis with the WZL software *ZaKo3D*, which is able to calculate the tooth root stresses of several gear types during meshing (Ref. 10). From these stresses and further parameters (e.g., local material properties) the tooth root load-carrying capacity is calculated in an approach based on the weakest link model of Weibull (Refs. 11–13).

After the local-based calculation method is validated, this method is used to derive a standard based calculation method for beveloid gears. The standard based calculation method uses analytic formulas to calculate the tooth root load carrying capacity of beveloid gears. In this method the tooth root stresses of be-

veloid gears are compared to the tooth root stresses of cylindrical gears. The effects which, observed during this comparison, are described and formulas are derived to take these effects into account.

Test Bench Trials

To detect the tooth root bending strength of a beveloid gear, a back-to-back test rig is used according to DIN 51354–Part 1, which uses the power circuit principle. The setup is illustrated in Figure 5. The tested beveloid gears are mounted in a gear box. They are connected by shafts to a transmission gear box. This setup is called power circuit. The test gear box is equipped with cylindrical gears. The cylindrical gears have the same gear data as the beveloids, but the cone angle is $\theta = 0^\circ$. The profile shift of the cylindrical gears is taken from the middle section of the beveloid gears. To avoid damage, the test gears are designed significantly wider

than the beveloid gears. It is possible to include a torque into the power circuit at the coupling which is mounted at one of the shafts. The other shaft is designed as torque shaft. An electric motor is used to drive the gears. Since the torque is realized by the power circuit, the motor only needs to apply power into the system that corresponds to the power losses due to, for example, friction.

The gear data of the test gears is presented in Figure 6 (left). To use the test principle of the back-to-back test rig according to DIN 51354, Part 1, parallel axes are used with a center distance of $a = 91.5$ mm. The module of the gears is $m_n = 2$ mm; the helix angle is $\beta_{1/2} = 3.024^\circ$; and the number of teeth are $z_{1/2} = 45/39$; further, the cone angle of Gear 1 is $\theta_1 = 3.6^\circ$. To realize parallel axes, the cone angle of Gear 2 is $\theta_2 = -3.6^\circ$.

The goal of the tests is to determine the fatigue limit of the test gears for a probability of survival of $P_S = 50\%$; the principle used is the staircase method according to Hück. In this method the test load is dependent on the result of the previous test run. The load is reduced at breakage and increased at run-out. In these tests the load step is fixed at $\Delta T_2 = 25$ Nm. A complete test run is reached if Gear 2 experiences $n_2 = 3,000,000$ load cycles without root breakage.

The results of the test are presented in Figure 6 (left). In the diagrams the test results are marked at the torque used in each test. The cross represents a breakage during the test; a filled circle represents test run-out. Invalid results are marked with a void circle. To take the test result of the last test (damage or test run-out) into account, a fictitious point is added after the last test. The fictitious point is marked with a void square. For the evaluation, all valid points and the fictitious point are used. This results in a torque for a probability of survival of 50% of $T_2 = 563.64$ Nm for Flank 1, and of $T_2 = 565.91$ Nm for Flank 2; the fatigue strengths of both flank sides are similar.

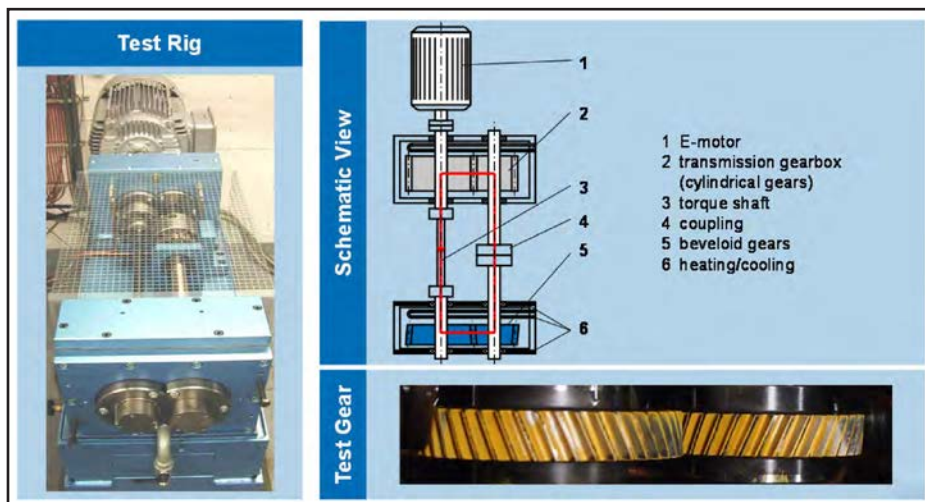
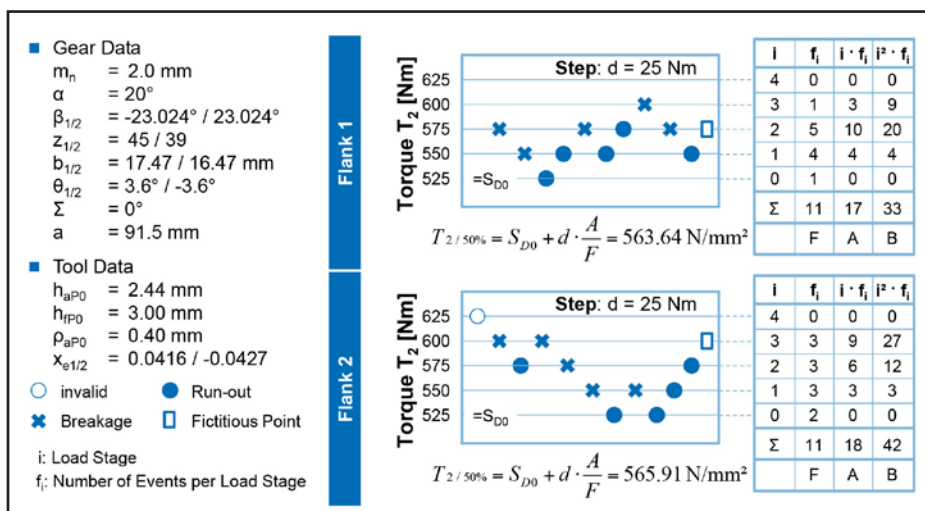


Figure 5 Back-to-back gear test rig according to DIN 51354, Part 1.



In the next section the calculation is presented briefly. This is followed by the application of the calculation method to the test gears that were already used for the test rig trials in the previous chapter.

Simulation method. In this approach three programs are used in sequence to calculate tooth root load-carrying capacity for beveloid gears. Figure 7 presents a brief overview of the three programs.

The first program in the simulation chain is the software *GearGenerator*, which calculates a 3D model of the beveloid gear via generating grinding simulation. The software is based on the calculation method of Röhrlingshöfer (Refs. 14, 1). The simulation uses the tool data, the gear data and the information about the axis setup of the machine (e.g., tilting or linked feeds) to calculate the tool geometry, the tool movements and, finally, the resulting gear geometry according to the laws of gearing (Ref. 15). A 3D model of the gear is provided as output. For the microgeometry analysis, the resulting geometry is compared to an ideally shaped involute and then plotted as profile and lead plot. Supplementing the manufacturing simulation, an algorithm was developed according to the Verein Deutscher Ingenieure (VDI) standard, VDI 2607 to evaluate the flank deviations (Refs. 16, 9). The excellent simulation accuracy of this method is shown by Röhrlingshöfer in Chapter 5.3.2 of his dissertation (Ref. 1).

The 3D models of the gears generated by *GearGenerator* are used as input for the tooth contact analysis software *ZaKo3D*. The general approach of *ZaKo3D* is the simulation of the 3D tooth contact. Therefore the geometric data of the flank and an FE model of a gear section are needed as input. Furthermore, pitch and assembly deviations can be considered. During the simulation the contact distances, loads, and deflections on the tooth are calculated. The results of the calculation can be displayed in established diagrams to support the gear designer during the development process.

The flank geometry is provided at the outset; in this work the geometry is taken from *GearGenerator*. Alternative input files, such as measurement data files from coordinate measurement machines, are possible as well. Regardless of the source of the input data, the flank must

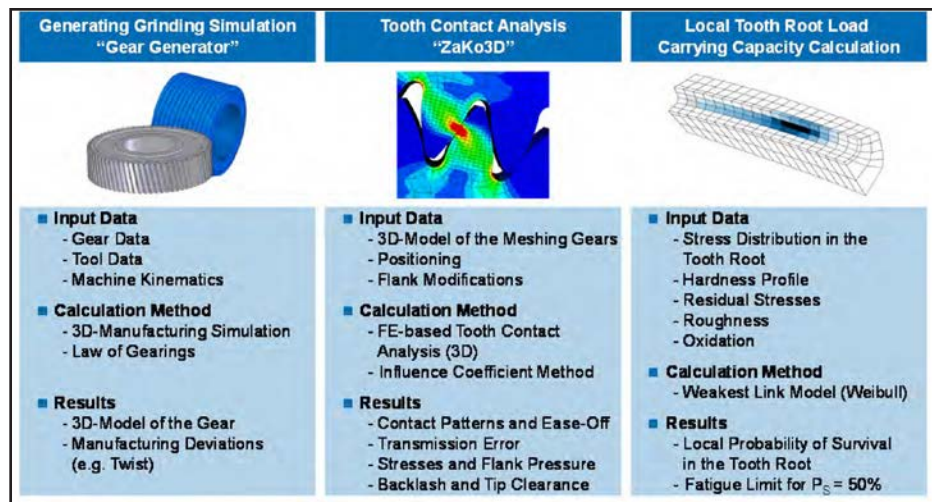


Figure 7 Simulation methodology (Ref. 13).

be defined by points in Cartesian coordinates and the direction of the normal vectors at each flank point.

In order to be able to simulate loaded condition, FE data has to be generated out of the flank data. The FE model contains the information about the stiffness of the gear; it is created by an automatic FE mesh generator for gear teeth (Ref. 10). The FE mesh generator needs the flank geometry to create the mesh. Furthermore, information about the FE node distribution inside the tooth is needed. Finally, the material properties must be defined. Each point of the modeled flanks is loaded with unit forces in each, x -, y - and z -direction. Using this model, a standard FE solver is used to calculate so-called influence coefficients. The influence coefficients hold the information about the deflection of all points during the application of each unit force. This contains the displacement influence coefficients α_i that are on the diagonal of the influence coefficient matrix, as well as the cross influence coefficients α_{ij} . To complete the input data, information about the positioning of the gears is needed. Different gear types can be positioned in *ZaKo3D*; e.g., spur gears, bevel gears, face gears and beveloid gears. The input of pitch deviations, microgeometry deviations and corrections, assembly deviations or different loads can be done by the user and is optional.

The tooth contact analysis starts with the calculation of the contact distances of the flanks during the mesh after reading the input data. This is done for the given number of rolling positions and for each flank point of all the flanks in contact. With these contact distances and

the information about the stiffness from the influence coefficients, a mathematic spring model is defined (Ref.18). Since the number of contact points in a rolling position and the force at each contact point influence each other, it is necessary to solve the spring model iteratively.

From these calculations the contact pattern and the transmission error can be derived load-free and under load. The transmission error of a gear is caused by geometric errors of the flanks (load-free content) and deflections (load content) of the gear, and gives a good impression of the dynamic gear excitation (Ref. 17). The course of the transmission error can be displayed over time and by performing a fast Fourier transformation in the frequency domain.

Using the forces on the nodes and the flank areas to which these forces are applied, the resulting pressure can be calculated. The flank area corresponding to a node is defined by the grid size (Ref. 18). The surface stress distribution on the flank has a major influence on the wear resistance of the flanks, and a reduction can lower the risk of pitting (surface fatigue) and improve the flank load-carrying capacity (Refs. 19–20). Furthermore, the ease-off, which represents the contact distances in the mesh area, is calculated load-free. This output data provides information about the gear behavior and can be used to predict the quality of the calculated gear design. This is necessary to reduce the needed number of design validation tests.

Tooth root stresses are calculated by *ZaKo3D* in an FE-based approach. The FE model, which is used for the influence

coefficient simulation, is applied with the forces that occur during discrete mesh positions. The stress tensors are calculated at each FE node in the whole root section and are evaluated according to several stress hypotheses (e.g., the von Mises stress hypothesis). The stress tensors can also be used to calculate the probability of survival in a local-based approach (Ref. 10).

The local-based calculation of the tooth root load-carrying capacity is based on the “weakest link” concept, invented by Waloddi Weibull. The weakest link concept says that not just the maximum stress must be taken into account for the fatigue determination; the distribution of weakest links in the material must be considered as well. In the weakest link concept the load stresses σ_a , the fatigue limit σ_D , the volume V and the Weibull module k (for the statistical distribution) are taken into account. The possibility to

apply the weakest link model to gears was first investigated by Dr. Brömsen and Dr. Zuber. In their dissertations the calculation of the 50% probability of survival PS/50% in pulsator tests is developed and verified (Refs. 21, 11, 12).

An FE model of the gear is used to calculate the tooth root load-carrying capacity of gears; input data are the stress tensors which were calculated in *ZaKo3D*. The material parameters — hardness, residual stresses and oxidation — are used in this method and the surface roughness in the root fillet is considered. With this input data the probability of survival P_S is calculated for each FE element. This is done by comparing the stress amplitude σ_a to the fatigue strength σ_D in the so-called integration points of the FE elements. The fatigue strength is calculated by empirical expressions from the material parameters. By numerical integration

this comparison is extended to the whole FE element. Multiplying the probabilities of survival of each FE element in the root equals the probability of survival of the total tooth root.

Application to the test gears. The method described in the previous section is applied to the gear used in the fatigue tests; the load is applied on Flank 2 (see Fig. 8). In the two diagrams at the top, the hardness profile and the residual stress profile used for the calculations are presented. For adjusting alignment errors and microgeometry corrections, the contact pattern was used. In the lower-left diagram the probability of survival is plotted over the torque at Gear 2. For low loads the probability of survival approaches $P_S = 1$. For high loads the probability of survival approaches $P_S = 0$. The probability of survival P_S drops significantly — between $T_2 = 500$ Nm and $T_2 = 600$ Nm. At approximately $T_2 = 576$ Nm, the probability of survival reaches 50%. In the test bench trials, described earlier, the torque $T_2 = 565.91$ Nm leads to a probability of survival of 50% (see Fig. 8, lower right). The difference between the simulation and the test rig results is lower than 2%. This shows the good correlation between simulation and testing. Hence it is possible to use the simulation to develop a standard-based approach.

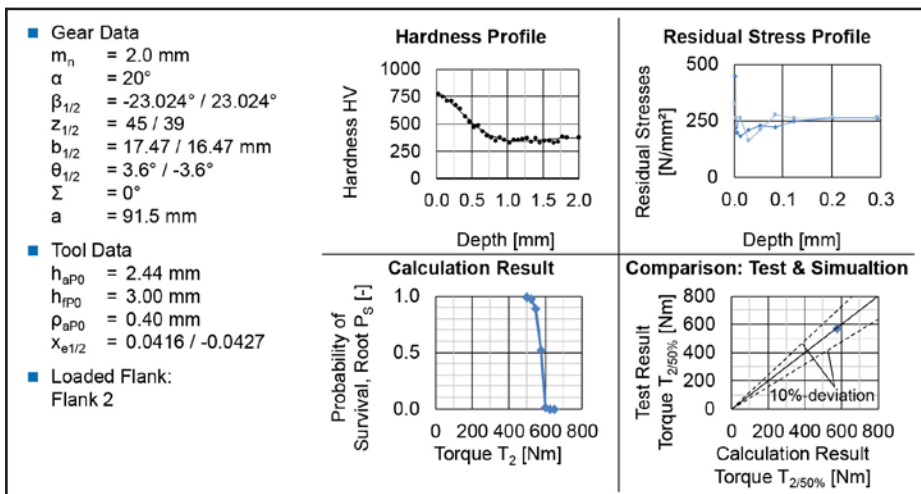


Figure 8 Application of local-based calculation method to a test gear.

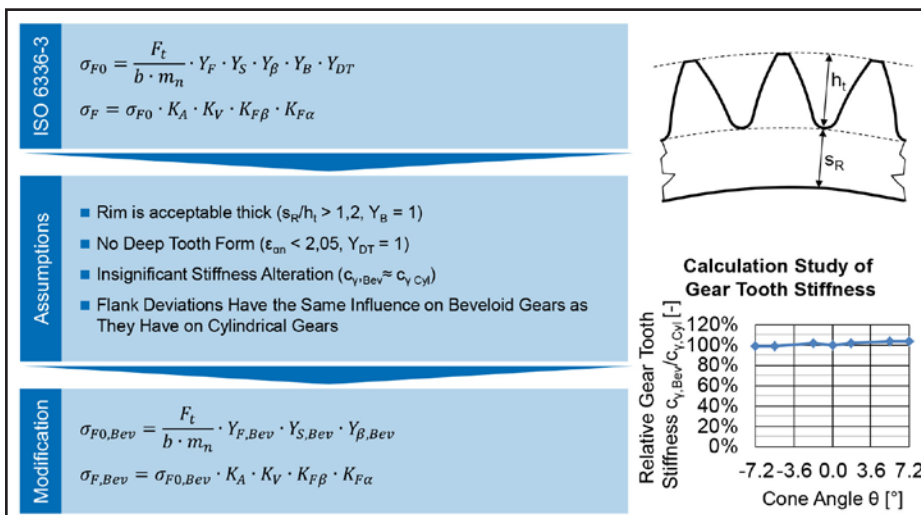


Figure 9 Analytical calculation for tooth root load carrying capacity of beveloid gears with parallel axes.

Standard-Based Calculation Method for Tooth Root Load-Carrying Capacity

Earlier it was shown that the stresses calculated in *ZaKo3D* can be used to calculate the tooth root load-carrying capacity of beveloid gears. Thus the software is used to develop a standard-based method for calculating tooth root stresses of beveloid gears. The approach of the standard-based calculation method is to use the existing calculation method of ISO 6336 by modifying its factors (Ref. 20). The approach for the modification is plotted in Figure 9 (left). In the upper part, the formula from ISO 6336 (Ref. 20) used to calculate the tooth root stress of cylindrical gears is presented. The Y - and K - factors, which are defined for cylindrical gear, have to be adapted to calculate tooth root stresses for beveloid gears.

In the approach presented, it is assumed that the rim is sufficiently thick

and that no deep tooth forms are investigated. Accordingly, the rim thickness factor YB and the deep tooth factor YDT have the value 1 and will not be considered further.

Under the assumption that helix angle deviations, profile corrections, and the pitch errors have the same effects for cylindrical gears and beveloid gears, and that the average gear stiffness of a beveloid and its derived cylindrical gear are similar, the formulas for the transverse load factor $KF\beta$, the face load factor $KF\alpha$ and the dynamic factor KV for the calculation of beveloid gears can be directly used from the standard calculation for cylindrical gears. Beveloid gears have been derived with cone angles between $\theta = -7.2^\circ$ and $\theta = 7.2^\circ$ from a cylindrical. For all versions the average tooth stiffness c_y has been calculated with *ZaKo3D*. In Figure 9, bottom right, the relationship between the average tooth stiffness of the beveloid variants $c_{y,Bev}$ and the relation of the average tooth stiffness of the cylindrical gears $c_{y,Cyl}$ is shown; only minor differences can be observed. The maximal deviation is 3.3%, so that the previously mentioned assumption of a similar average tooth stiffness of cylindrical gears and beveloid gears is achieved.

The application factor K_A depends only on the engine and the load of the gear box. The factor can be transferred from the calculation method of cylindrical gears into the calculation method of beveloid gears without any adaptation.

What remains are the form factor Y_F , the stress correction factor Y_S and the helix angle factor Y_β ; these are related to the geometry and the contact conditions. Due to the significant changes between cylindrical gears and beveloid gears, the factors are redefined. In the next section, these geometry-dependent factors for beveloid gears are developed. Included are the beveloid form factor $Y_{F,Bev}$ and the beveloid stress correction factor $Y_{S,Bev}$. After these the influence of the overlap ratio and of the helix angle on the tooth root stress of beveloid gears are specified by the beveloid helix angle factor $Y_{\beta,Bev}$ later sections of this paper.

Form factor $Y_{F,Bev}$ and stress correction factor $Y_{S,Bev}$ Beveloid gears change their profile shift with the tooth width (Ref. 1). That results in changes of the cross-section of the gearing and the notch in the

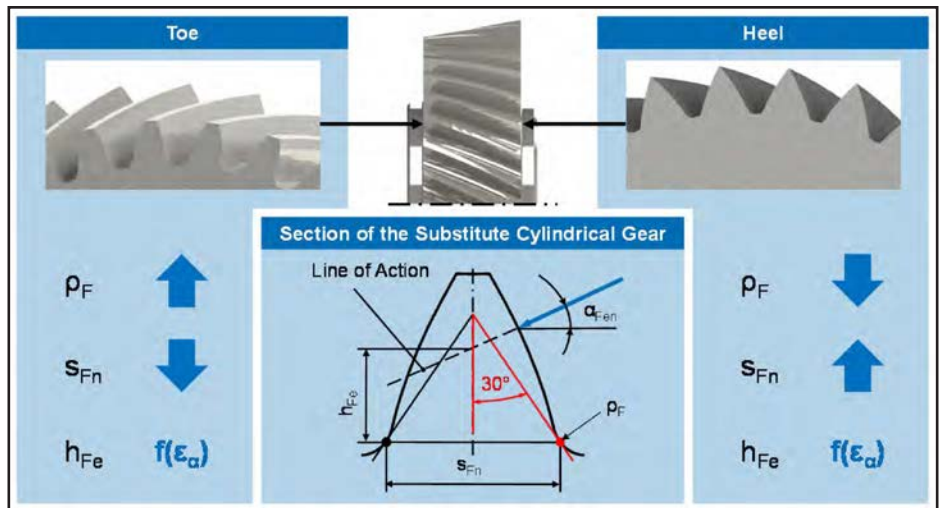


Figure 10 Determining values for the calculation of the beveloid form factor $Y_{F,Bev}$ and the beveloid stress correction factor $Y_{S,Bev}$

tooth root. Figure 10 shows a beveloid gear that illustrates that relationship. On the left side, the beveloid gear face side with a low profile shift is illustrated. On that face side thin tooth roots with a small normal chord s_{Fn} occur. Furthermore, the curvature of the tooth root curve is low; therefore the root radius ρ_F on that face side is high. The right side shows the beveloid gear's face side with a high profile shift. On that side the teeth are thick, which results in a long normal chord s_{Fn} . The root curve displays a low root radius ρ_F . The bending moment arm h_{Fe} for load incidence at the outer point of contact depends on the transverse contact ratio ϵ_α . This depends on several factors, which make a simple statement about the relative change of the profile shift impossible.

To detect the influence from the varying transverse sections on the tooth root stresses, the profile shift at the axial coordinate with the maximal tooth root stresses is used. First, this is determined in FE calculations. The estimation by analytical equations has to be developed.

Supplied with the data of the face section of the maximal tooth root stress, a cylindrical, substitute helical gear is generated that is used to determine the helix angle factor and the stress correction factor. Since these depend on the profile shift of the critical face section, they are called beveloid form factor $Y_{F,Bev}$ and beveloid stress correction factor $Y_{S,Bev}$.

Helix factor, Y_β . The contact conditions of beveloid gears with parallel axes are significantly different from the contact conditions of cylindrical gears (Refs. 22, 2). The differences are illustrated

in Figure 11 by comparing the fields of action of both gear types. The left side shows the field of action of a helical cylindrical gear; the field of action is rectangular. The width is limited by the active tooth width b of both gears. The length is formed by the root and the tip length of engagement. The lines of contact are shown as dashed lines and are inclined at the base helix angle within the field of action. In direction of the length of engagement, the distance of the lines of action is described by the transverse base pitch on the path of contact p_{et} . The overlap ratio ϵ_β is calculated with Equation 1 from the tooth width b , the base helix angle β_b and the transverse base pitch on the path of contact p_{et} (Ref. 23):

$$\epsilon_\beta = \frac{b \tan \beta_b}{p_{et}} \quad (1)$$

where

- ϵ_β is overlap ratio
- b is (active) tooth width, mm
- β_b is base helix angle, degrees
- p_{et} is transverse base pitch on the path of contact, mm

The right side of Figure 11 shows a field of action of a helical beveloid gear. Like cylindrical gears, the width of the field of action is limited by the active tooth width b . However, different tip and root lines of action on the face sections lead to a parallelogram-shaped field of action. For a fully accurate illustration of the field of action, the boundaries at the inlet and outlet must be drawn hyperbolically (Ref. 23). The curvatures of hyperbolas of conical spur gears are usually so small that they can be replaced

by straight lines. The lines of action are in the field of action diagonally, as it is observed for helical cylindrical gears, but for the fact that the base helix angle on the right flank $\beta_{b,R}$ and the base helix angle of the left flank $\beta_{b,L}$ differ from each other (Ref. 22).

The overlap ratio of beveloid gears is composed of two parts. The first component is the overlap angle of the flank lines $\varphi_{\beta R,L}$. This describes the angle that is enclosed by the axial planes at the endpoints of the flank lines. This part of the overlap ratio is calculated analogous to cylindrical gears (Eq. 2). For beveloid gears, the helix angles on the right and left flank must be considered, dependent on the flank side, so that the overlap angle is calculated separately for both sides. The second part is the overlap angle of the field of action $\varphi_{FMR,L}$. The field of action is inclined at the angles $\beta_{FRf,L}$ and $\beta_{FaR,L}$ on the entry and on the exit side (Fig. 11). This results in the field

entry overlap angle $\varphi_{FMR,L}$ and the field exit overlap angle $\varphi_{FMR,L}$ (Eqs. 3, 4). The overlap angle of the field of action $\varphi_{FMR,L}$ is determined by the average of the field entry overlap angle $\varphi_{FRf,L}$ and the field exit overlap angles $\varphi_{FaR,L}$ (Ref. 22).

$$\varphi_{\beta R,L} = \frac{2b \tan \beta_{bR,L}}{d_{bR,L}} \tag{2}$$

$$\varphi_{FRf,L} = \frac{2b \tan \beta_{FRf,L}}{d_{bR,L}} \tag{3}$$

$$\varphi_{FaR,L} = \frac{2b \tan \beta_{FaR,L}}{d_{bR,L}} \tag{4}$$

where

$\varphi_{\beta R,L}$ is overlap angle of the flank line, degrees

b is (active) tooth width, mm

$\beta_{bR,L}$ is base helix angle, degrees

$d_{bR,L}$ is base circle diameter, mm

$\varphi_{FRf,L}$ is field entry overlap angles, degrees

$\varphi_{FaR,L}$ is field exit overlap angles, degrees

$\beta_{FRf,L}$ is field entry inclination angle, degrees

$\beta_{FaR,L}$ is field exit inclination angle, degrees

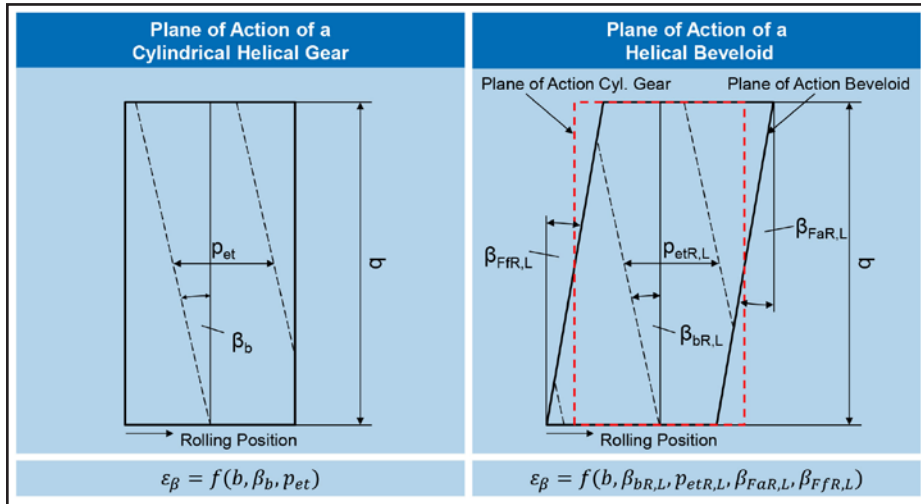


Figure 11 Calculation of overlap ratio of beveloids.

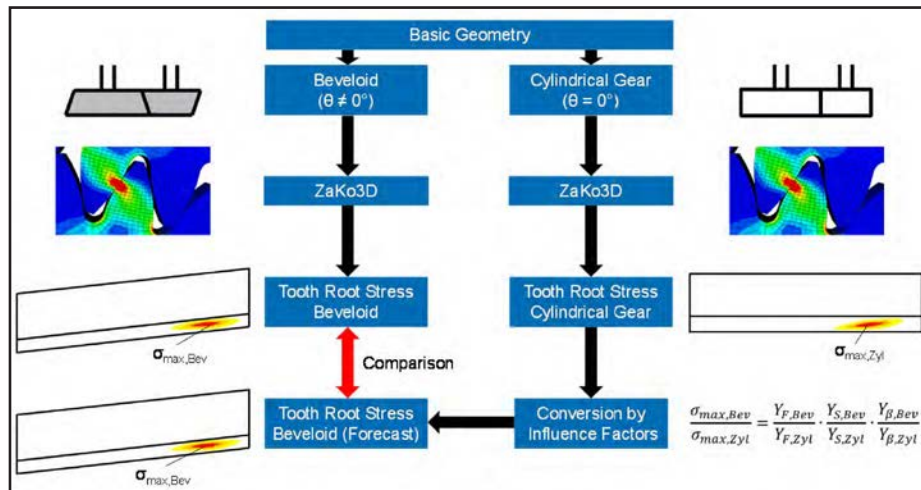


Figure 12 Method for investigation of beveloid factors.

$\beta_{FaR,L}$ is field exit inclination angle, degrees

The overlap ratio of beveloid gears with parallel axis is calculated with Equation 5 by the difference between the overlap angle of the flank lines $\varphi_{\beta R,L}$ and the mean field overlap angle $\varphi_{FMR,L}$, divided by the angular pitch τ , which is calculated according to Equation 6 (Ref. 22). Depending on orientation of the base helix angle of the line of action, the contact ratio can be increased or decreased. This relation can be observed by comparing the field of action of a beveloid gear and the field of action of a cylindrical gear. On the right section of Figure 11, the field of action of a beveloid gear and the field of action of a cylindrical gear with the data of the middle transverse section are superimposed. It is shown that the contact at the beveloid gear starts earlier due to the helix angle of the field of action at the inlet side $\beta_{FRf,L}$ and the contact at the beveloid gear ends later due to the helix angle of the field of action at the outlet side $\beta_{FaR,L}$. The contact ratio is consequently higher than the contact ratio of a cylindrical gear; however, if the helix angle is more right-oriented, than left so, the relationship then changes and smaller contact ratio occurs for the beveloid gear.

$$\epsilon_{\beta,BevR,L} = \frac{\varphi_{\beta R,L} - \varphi_{MR,L}}{\tau} \tag{5}$$

$$\tau = \frac{2\pi}{z} \tag{6}$$

where

$\epsilon_{\beta,BevR,L}$ is overlap ratio (beveloid)

$\varphi_{\beta R,L}$ is overlap angle of the flank line, degrees

$\varphi_{MR,L}$ is mean field overlap angle, degrees

τ is pitch angle, degrees

z is number of teeth

The calculation of the beveloid helix factor $Y_{\beta,BevR,L}$ for beveloid gears is analogous to the calculation of the contact ratio factor of a cylindrical gear. For the overlap ratio, the beveloid helix factor of beveloid gears according to Equation 5 is used. The helix angle of the appropriate flank side is used since the contact ratio and the helix angle usually differ for both flank sides. The beveloid helix factor $Y_{\beta,BevR,L}$ must also be calculated separately for each flank.

$$Y_{\beta,BevR,L} = 1 - \epsilon_{\beta,BevR,L} \frac{\beta_{R,L}}{120} \tag{7}$$

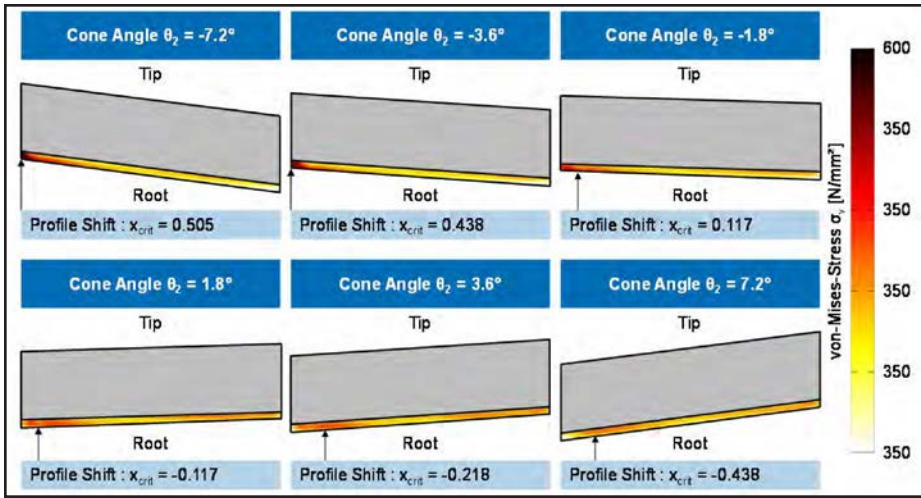


Figure 13 Stress maxima position of the sample gear in dependence of the cone angle (torque $T_2=475$ Nm).

where

- $Y_{\beta,Bev,R,L}$ is beveloid helix factor
- $\beta_{R,L}$ is helix angle, degrees
- $\epsilon_{\beta,Bev,R,L}$ is overlap ratio (beveloid)

Application to a sample gear. The calculation method presented earlier in this paper will be applied to two sample gears in the following paragraphs. A detailed analysis of the individual calculation factors and their combinations will be performed. The strategy in order to do so is shown in Figure 12.

Basic geometry will be defined for a test gear. From that basic geometry a cylindrical gear — also described as a beveloid gear with the cone angle $\theta=0^\circ$ — as well as several beveloid gears with parallel axes — will be derived. For all variants the maximum tooth root stresses will be calculated with *ZaKo3D*. Subsequently a conversion of the tooth root stress of the cylindrical gear into the tooth root stress of the derived beveloid gear will be performed using the approach presented earlier in this paper. Those calculated tooth root stresses will be compared to the results from *ZaKo3D*.

The sample gear to which the calculation method will be applied has the following gear data: The normal module is $m_n=2$ mm and the helix angle is $\beta=23.024^\circ$. The cone angle will be varied between $\theta=-7.2^\circ$ and $\theta=7.2^\circ$. Gear 2 has a face width of $b_2=16.0$ mm, which is narrower than Gear 1, with a face width of $b_1=16.8$ mm.

For all variants a tooth contact analysis with *ZaKo3D* was performed. The model used to calculate the tooth root stresses in *ZaKo3D* has a flank resolution of 30 grid

points in profile direction and 30 grid points in flank direction for Gear 1. Gear 2 has a flank resolution of 31 grid points in profile direction and 31 grid points in flank direction.

The gearing will be loaded with a torque of $T_2=475$ Nm on Gear 2. In the whole tooth root area the tooth root stresses will be evaluated at the FE nodes according to the von Mises criteria. In Figure 13 the maxima of the von Mises-equivalent stress throughout the whole tooth root area for some of the sample gearings with the considered cone angles are shown. The place where the maximum von-Mises-equivalent stress appears is indicated by an arrow. For all variants this place is located on the left of the tooth flank. The maximum tooth root stresses are located directly at the heel for the variants with negative cone angles. Note that with increasing cone angle the maximum stress location moves slightly towards the center of the gearing.

The face section with the maximum tooth root stresses are used to calculate the factors $Y_{F,Bev}$ and $Y_{F,Cyl}$ for all variants for the following calculations: the face sections differ in the addendum modifications x_1 and x_2 and in the tip circle diameters d_{a1} and d_{a2} of gear and pinion. As the tip circle diameter is related to the addendum modification through the addendum factor, only the corresponding addendum modification will be listed.

In order to evaluate the influence of the Y factors on the calculation of the tooth root stresses, a conversion of the maximum tooth root stress of a cylindrical gear to the maximum tooth root stress

of the beveloid variants was performed. The converted stresses were compared to the calculated tooth root stresses of *ZaKo3D*. The conversion is described through Equation 8. In the following the single factors of Equation 8 as well as combinations of those factors are examined. Thereby other factors shall not be considered. The respective fractions were deleted from Equation 8.

$$\frac{\sigma_{v,2Bev}}{\sigma_{v,2Cyl}} = \frac{Y_{F,Bev}}{Y_{F,Cyl}} \frac{Y_{S,Bev}}{Y_{S,Cyl}} \frac{Y_{\beta,Bev}}{Y_{\beta,Cyl}} \quad (8)$$

where

$\sigma_{v,2Bev}$ is maximum Von-Mises-Stress in the beveloid tooth root, N/mm²

$\sigma_{v,2Cyl}$ is maximum Von-Mises-Stress in the cylindrical gear's tooth root, N/mm²

$Y_{F,Bev}$ is beveloid form factor

$Y_{F,Cyl}$ is form factor

$Y_{S,Bev}$ is beveloid stress correction factor

$Y_{S,Cyl}$ is stress correction factor

$Y_{\beta,Bev}$ is beveloid helix factor

$Y_{\beta,Cyl}$ is helix factor

In the upper left diagram of Figure 14, the tooth root stresses calculated with *ZaKo3D* are compared to the tooth root stresses calculated with Equation 8; here all Y-factors are considered. With the helix factor Y_{β} , the dependence of the maximum tooth root stress on the cone angle turns out to have a contrary course between the predicted maximum tooth root stresses and the ones calculated with *ZaKo3D*. Due to that, the combination of all factors is inappropriate in order to predict the maximum tooth root stresses for the considered beveloid gears.

In the three remaining plots in Figure 14, only two of the three possible Y-factors are taken into consideration. In the upper right diagram the calculation of the tooth root stresses of the beveloid variants is performed on the basis of the tooth root stresses of the cylindrical gear $\sigma_{v,2,Cyl}$, the form factor YF , and the stress correction factor Y_S . In the range of negative cone angles, the tooth root stress are predicted considerably lower than in the calculation with *ZaKo3D*. In the range of positive cone angles, higher tooth root stresses are predicted than were calculated with *ZaKo3D*. However, the deviations are small. Due to the underestimation of the tooth root stresses for negative cone angles, the combination of the form factor Y_F and the stress correction factor Y_S is not sufficient to predict the tooth root

stresses of the considered beveloid variants.

In the diagram on the lower left hand side the conversion of the tooth root stresses is performed on the basis of the tooth root stresses of the cylindrical gear $\sigma_{v,2,Cyl}$, the form factor Y_F and the helix factor Y_β . The relationship between cone angle and maximum tooth root stresses shows strongly contrary tendencies. Hence combination of form factor Y_F and stress correction factor Y_S is not sufficient to predict the tooth root stresses of the considered beveloid variants.

In the lower right hand diagram the conversion of the tooth root stresses is performed on the basis of the tooth root stresses of the cylindrical gear $\sigma_{v,2,Cyl}$, the stress correction factor Y_S and the helix factor Y_β . The tooth root stresses being calculated through the conversion match the tooth root stresses calculated with *ZaKo3D* very well; the maximum deviation is 2.33%. Consequently the combination of the stress correction factor Y_S and helix factor Y_β suits very well in order to calculate the maximum tooth root stresses of the considered beveloid variants from the tooth root stresses of the cylindrical gear version $\sigma_{v,2,Cyl}$.

Conclusion

Earlier in this paper, an investigation into which *Y*-factors allow a conversion of the tooth root stresses of a cylindrical gear to the tooth root stresses of a beveloid gear with a high accordance to the calculation results of *ZaKo3D*. The highest accordance to the results of *ZaKo3D* is achieved if the stress correction factors Y_S and the helix factor Y_β are used in the conversion while the form factor Y_F is not taken into consideration.

Due to the high accordance with the sample gears the conversion performed on the basis of the stress correction factor

Y_S and the helix factor Y_β in order to calculate the tooth root stresses of beveloids will be added to the calculation method. The form factor Y_F will furthermore be deducted from the data of the average transverse section. Under the boundary conditions described earlier, the calculation method for the tooth root stresses of beveloids results in Equations 9 and 10: (9)

$$\sigma_{F0,Bev} = \frac{F_t}{m_n b} Y_{F,Z\beta} Y_{S,Bev} Y_{\beta,Bev} \tag{10}$$

$$\sigma_{F,Bev} = \sigma_{F0,Bev} K_A K_V K_{F\beta} K_{F\alpha}$$

where

$\sigma_{F0,Bev}$ is nominal tooth stress, N/mm²

F_t is nominal tangential load, N

b is tooth width, mm

m_n is normal module, mm

$Y_{F,Z\beta}$ is form factor (mean transverse section)

$Y_{S,Bev}$ is beveloid stress correction factor (critical transverse section)

$Y_{\beta,Bev}$ is beveloid helix factor

$\sigma_{F,Bev}$ is tooth root stress, N/mm²

K_A is application factor;

K_V is dynamic factor;

$K_{F\beta}$ is face load factor;

$K_{F\alpha}$ is transverse load factor.

An important part of calculating the form factor is the calculation of the tooth root critical section with the tooth root normal chord s_{Fn} and the tooth width b . High addendum modifications, as they appear at a beveloid's heel, result in long tooth root normal chords and therefore a high section modulus of the cross-section. Low addendum modifications, as they appear at a beveloid's toe, result in short tooth root normal chords and a low section modulus. With beveloids, the profile shift changes alongside the tooth width. Therefore the length of the tooth root normal chords changes along the cross-section. This is outlined by a trapezoidal cross-section of the beveloid at a section through the tooth root (Fig. 15). This is compared to the cross-section of a substitute gear with the gear data of the heel and a substitute gear with the gear data of the toe.

The gear data of the heel lead to an overestimation of the section modulus, while the toe's section modulus is low. The use of the gear data of the average cross-section offers a good approach to approximate the section modulus of a beveloid gearing. This approach will require further investigation.

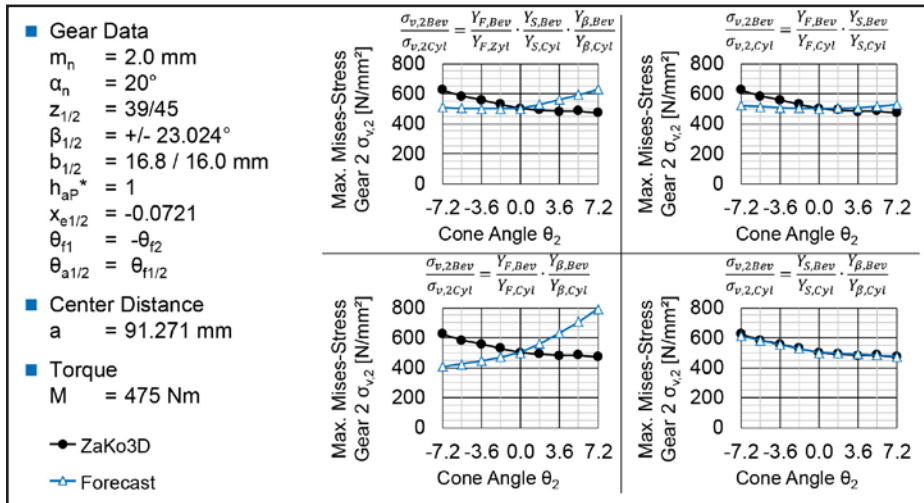


Figure 14 Influence of the *Y*-factors on the tooth root stress calculation.

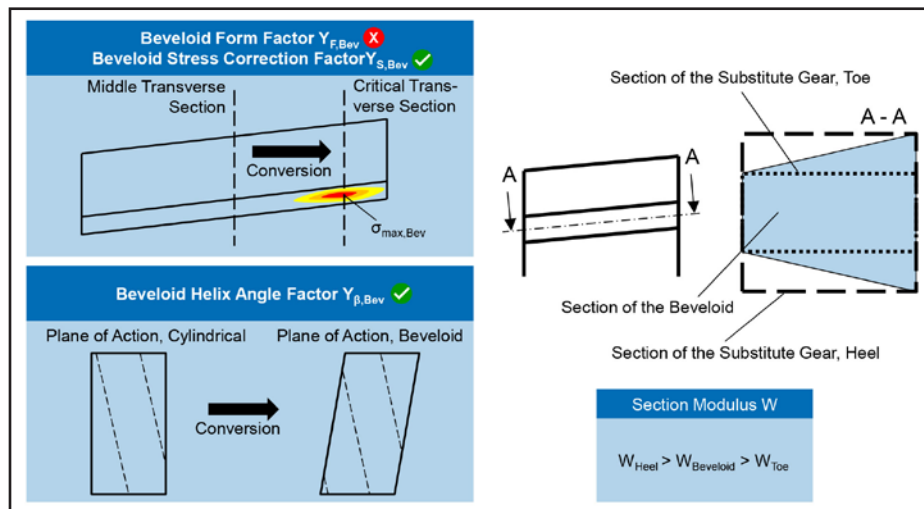


Figure 15 Conclusion.

Summary and outlook

In this paper, two developed methods for the tooth root load-carrying capacity calculation for beveloid gears with parallel axes are presented. The first method calculates the tooth root load-carrying capacity in an FE-based approach. The model is used to calculate the tooth root load-carrying capacity of a test gear. The results show good correlation to investigations on a back-to-back test rig.

The second method uses analytic formulas to calculate the tooth root load-carrying capacity of beveloid gears. In this method the tooth root load-carrying capacity of beveloid gears is compared to the tooth root load-carrying capacity of conventional cylindrical gears. The effects observed during this comparison are described and formulas are derived to take these effects into account.

The new method submits changes on three *Y*-factors. The presented method shows for the sample gear a good correlation. A validation on further cases has not been made yet. To define a method for an extensive scope more comparisons on further gear cases are scheduled.

Furthermore, the method introduced here is presently based on a numerical calculation of the location of the maximum tooth root stresses. To provide a closed analytical solution, the method has to be expanded by an analytical forecast of the location of the maximum tooth stresses. Finally, further verification tests are necessary to confirm whether the analytical calculation — especially the differences in the loads of the flank — can give indication of the influence of the cone angle on the stress distribution. ⚙️

References:

1. Röthlingshöfer, T. "Auslegungsmethodik zur Optimierung des Einsatzverhaltens von Beveloidverzahnungen," Dissertation, RWTH Aachen, 2012.
2. Roth, K. Zahnradtechnik, "Evolventen-Sondervverzahnungen zur Getriebeverbesserung," Springer, Berlin, 1998.
3. Winkler, T. "Untersuchungen zur Belastbarkeit Hohlkorrigierter Beveloidgetriebe für Schiffsgetriebe mittlerer Leistung" Dissertation, Universität Stuttgart, 2002.
4. Zhu, C., C. Song, T. Lim, and S. Vijayaraj. "Geometry Design and Tooth Contact Analysis of Crossed Beveloid Gears for Marine Transmissions," *Chinese Journal of Mechanical Engineering*, Bd. 25, Nr. 2, S. 328–337, 2012.
5. Wagner, M. "Beitrag zur Geometrischen Auslegung von Stirnradpaarungen mit Kleinen Achskreuzungswinkeln," Dissertation, Universität Stuttgart, 1993.

6. Börner, J., K. Humm, K. and F. J. Joachim. "Development of Conical Involute Gears (Beveloids) for Vehicle Transmissions," *Gear Technology*, Nr. 6, S. 28–35, 2005.
7. Alxneit, H. "Optimierung des Übertragungsverhaltens Konischer Außenstirnräder mit Kreuzenden Achsen," Dissertation, Universität Stuttgart, 2010.
8. Weck, M. and C. Brecher. "Werkzeugmaschinen," Springer, Berlin (U.A.), 2005.
9. Brecher, C., M. Brumm, F. Hübner and J. Henser. "Influence of the Manufacturing Method on the Running Behavior of Beveloid Gears," *Production Engineering*, Bd. 7, Nr. 2-3, S. 265–274, 2013.
10. Brecher, C., M. Brumm, and J. Henser. "Simulation von Beveloidverzahnungen — Berechnung der Zahnfußspannungen," DMK 2011: *Dresdner Maschinenelemente Kolloquium*, 29-30, November 2011, 2011.
11. Brömsen, O. "Steigerung der Zahnfußtragfähigkeit von Einsatzgehärteten Stirnrädern durch Rechnerische Zahnfußoptimierung," Dissertation, RWTH Aachen, Shaker, Aachen, 2005.
12. Zuber, D. Fußtragfähigkeit Einsatzgehärteter Zahnräder unter Berücksichtigung Lokaler Materialeigenschaften, Shaker, Aachen, 2008.
13. Brecher, C., M. Brumm and J. Henser. "Local Approach for the Evaluation of Tooth Root Load Carrying Capacity of Beveloid Gears," *Fourth WZL Gear Conference*, Schaumburg, Illinois, 2012.
14. Brecher, C., T. Röthlingshöfer and C. Gorgels. "Manufacturing Simulation of Beveloid Gears for the Use in a General Tooth Contact Analysis Software," *Production Engineering*, Bd. 3, Nr. 1, S. 103–109, 2009.
15. Litvin, F. L. *Gear Geometry and Applied Theory*, PTR Prentice Hall, Englewood Cliffs, N.J., 1994.
16. VDI 2607. "Computer-Aided Evaluation of Profile and Helix Measurements on Cylindrical Gears with Involute Profile," Beuth Verlag, Berlin, 2000.
17. Smith, J. D. *Gear Noise and Vibration*, Marcel Dekker Inc., New York, 2003.
18. Hemmelmann, J. E. "Simulation des Lastfreien und Belasteten Zahneingriffs zur Analyse der Drehübertragung von Zahnradgetrieben," Dissertation, RWTH Aachen, Shaker, Aachen, 2007.
19. Niemann, G., H. Winter and B. -R. Höhn. *Maschinenelemente. Konstruktion und Berechnung von Verbindungen, Lagern, Wellen. Konstruktion und Berechnung von Verbindungen, Lagern, Wellen*, 2005.
20. ISO 6336: *Calculation of Load Capacity of Spur and Helical Gears*; 2007.
21. Weibull, W. *A Statistical Theory of the Strength of Materials*, Ingeniörsvetenskapsakademiens Handlingar, Bd. 151, Generalstabens Litografiska Anstalts Förlag, Stockholm, 1939.
22. Zierau, S. "Die Geometrische Auslegung Konischer Zahnräder und Paarungen mit Parallelen Achsen," Dissertation, Technische Universität Braunschweig, 1993.
23. DIN 3960: Begriffe und Bestimmungsgrößen für Stirnräder (Zylinderräder) und Stirnradpaare (Zylinderradpaare) mit Evolventenverzahnung; Beuth Verlag, Berlin, 1987.
24. Haupt, U. "Keilschrägverzahnung für Getriebe mit Einstellbarem Verdrehlankenspiel," Dissertation, TU Braunschweig, 1981.

Prof. Dr.-Ing. Christian Brecher



Prof. Dr.-Ing. Christian Brecher has since 2004 served as Ordinary Professor for Machine Tools at the Laboratory for Machine Tools and Production Engineering (WZL) of the RWTH Aachen, as well as director of the Department for Production Machines at the Fraunhofer Institute for Production Technology IPT. Upon receipt of his engineering degree he began his career as a research assistant and later as team leader in the Department for Machine Investigation and Evaluation at the WZL. From 1999–2001 Brecher worked as a senior engineer with responsibility for machine tools and director (2001–2003) for development and construction at the DS Technologie Werkzeugmaschinenbau GmbH, Mönchengladbach. Brecher has received numerous honors and awards, the Springorum Commemorative Coin and the Borchers Medal of the RWTH Aachen among them.

Markus Brumm, an RWTH graduate with a degree in mechanical engineering, began his career in 2005 as a research assistant in gear investigation at the Laboratory for Machine Tools and Production Engineering (WZL) of the RWTH Aachen. He subsequently became that group's team leader in 2010.



Jannik Henser has studied mechanical engineering at RWTH Aachen University in Germany. During his studies he worked for four years as student assistant at the Laboratory for Machine Tools and Production Engineering (WZL) of RWTH Aachen University and interned at the iron powder manufacturer Höganäs AB in Sweden. He finished his studies successfully in 2010 with the diploma thesis "Micro Geometry Optimization of Powder Metal Gears" and started working as a PhD-student at WZL Gear Department for Prof. C. Brecher. His fields of research are tooth contact analysis, tooth root load-carrying capacity and beveloid gears. More than 10 papers were published on conferences and in journals under his direction.

